Article

Cell Reports

Islet Coordinately Regulates Motor Axon Guidance and Dendrite Targeting through the Frazzled/DCC Receptor

Graphical Abstract

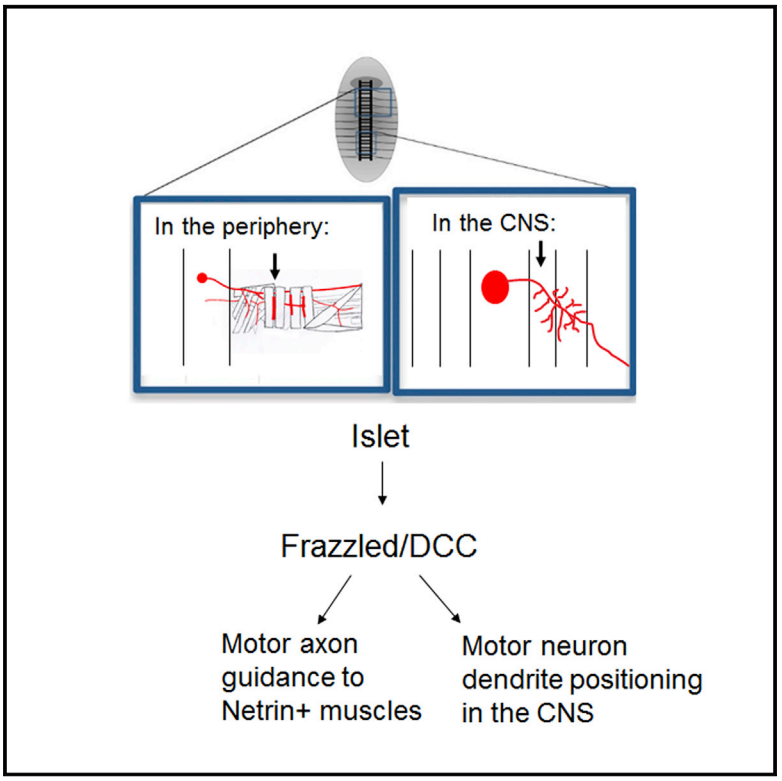

Authors

Celine Santiago, Greg J. Bashaw

Correspondence

gbashaw@mail.med.upenn.edu

In Brief

How individual transcription factors establish multiple aspects of neuronal identity remains poorly understood. Santiago and Bashaw find that the Islet transcription factor coordinately regulates two essential aspects of motor neuron morphology, axon and dendrite position, through a single downstream effector, the guidance receptor Frazzled/DCC.

Highlights

- Islet is required for *fra* expression in a subset of motor neurons
- Islet overexpression induces *fra* expression and a *fra*-dependent phenotype
- *Isl* and *fra* are required for axon and dendrite targeting in motor neurons
- Overexpression of Fra rescues motor axon and dendrite targeting in *isl* mutants

Santiago & Bashaw, 2017, Cell Reports *18*, 1646–1659
February 14, 2017 © 2017 The Author(s).
http://dx.doi.org/10.1016/j.celrep.2017.01.041

OPEN ACCESS
CellPress

Cell Reports
Article

Islet Coordinately Regulates Motor Axon Guidance and Dendrite Targeting through the Frazzled/DCC Receptor

Celine Santiago[1] and Greg J. Bashaw[1,2,*]
[1]Department of Neuroscience, Perelman School of Medicine, University of Pennsylvania, Philadelphia, PA 19104, USA
[2]Lead Contact
*Correspondence: gbashaw@mail.med.upenn.edu
http://dx.doi.org/10.1016/j.celrep.2017.01.041

SUMMARY

Motor neuron axon targeting in the periphery is correlated with the positions of motor neuron inputs in the CNS, but how these processes are coordinated to form a myotopic map remains poorly understood. We show that the LIM homeodomain factor Islet (Isl) controls targeting of both axons and dendrites in *Drosophila* motor neurons through regulation of the Frazzled (Fra)/DCC receptor. Isl is required for *fra* expression in ventrally projecting motor neurons, and *isl* and *fra* mutants have similar axon guidance defects. Single-cell labeling indicates that *isl* and *fra* are also required for dendrite targeting in a subset of motor neurons. Finally, overexpression of Fra rescues axon and dendrite targeting defects in *isl* mutants. These results indicate that Fra acts downstream of Isl in both the periphery and the CNS, demonstrating how a single regulatory relationship is used in multiple cellular compartments to coordinate neural circuit wiring.

INTRODUCTION

The diversity of cell types is one of the nervous system's most remarkable features, and understanding how this diversity is achieved remains a major challenge. Many studies have shown that combinations of transcription factors act in a cell-type-specific manner to specify a neuron's morphological and functional properties (Corty et al., 2009; Hobert, 2015). The regulation of axon and dendrite targeting is key to determining a neuron's connectivity and is controlled through the combined action of guidance receptors, adhesion molecules, and cytoskeletal regulators (Lefebvre et al., 2015; O'Donnell et al., 2009). Although recent studies have begun to delineate relationships between these cellular effectors and the transcription factors that control their expression, it remains unclear to what extent individual transcription factors regulate multiple aspects of neural morphogenesis (Santiago and Bashaw, 2014). In particular, although several factors have been shown to control both axon and dendrite development, whether they do so through shared or distinct targets is unknown. In mice, the target-induced E26 transformation-specific (ETS) factor Pea3 (Etv4) is required for axonal branching in a subset of limb-innervating neurons and for the position and connectivity of motor neuron dendrites in the spinal cord (Livet et al., 2002; Vrieseling and Arber, 2006). In the *Drosophila* olfactory system, the Pit-Oct-Unc (POU) factor Acj6 is required in a subset of projection neurons both for axonal branching in the lateral horn and for dendrite targeting in the antennal lobe (Komiyama et al., 2003). However, in these and other examples, the downstream programs that mediate the effects of these transcription factors on axon and dendrite targeting remain unidentified.

In the *Drosophila* larval and adult nervous systems, motor neuron dendrites form within stereotyped medio-lateral regions in the CNS that correlate with cell identity and with the position of motor axons in the periphery (Baek and Mann, 2009; Brierley et al., 2009; Mauss et al., 2009). Slit-Roundabout (Robo) and Netrin-Fra signaling are key regulators of dendrite targeting, and manipulating the levels of Robo1 or Fra causes shifts in dendrite position, suggesting that these receptors act in a cell-autonomous manner (Brierley et al., 2009; Mauss et al., 2009).

In adult motor neurons, birth order correlates with dendrite position, suggesting the involvement of a temporal code of transcription factors (Brierley et al., 2009). There is no indication that birth order plays a role in dendrite targeting in the embryo (Mauss et al., 2009); instead, the correlation between the dorsal-ventral position of axons and the medio-lateral position of dendrites suggests the intriguing hypothesis that the same factors that specify dorsal-ventral axon guidance decisions may also regulate dendrite position. Taken together, these data suggest that subset-specific transcription factors regulate dendrite targeting through their effects on *fra*, *robo1*, or genes in those pathways in *Drosophila* motor neurons. However, this model remains untested.

The well-conserved transcription factors Even-skipped (Eve), Hb9, Islet (Isl), and Lim3 are expressed in restricted subsets of embryonic motor neurons and have been extensively studied in the context of axon guidance, but whether the same transcriptional regulators control dendrite development is not known (Broihier and Skeath, 2002; Fujioka et al., 2003; Labrador et al., 2005; Landgraf et al., 1999; Odden et al., 2002; Thor and Thomas, 1997; Thor et al., 1999). We have shown previously that Hb9 acts through the Robo2 receptor to regulate axon guidance in RP3 neurons, a subset of ventrally projecting motor

 © 2017 The Author(s).
This is an open access article under the CC BY-NC-ND license (http://creativecommons.org/licenses/by-nc-nd/4.0/).

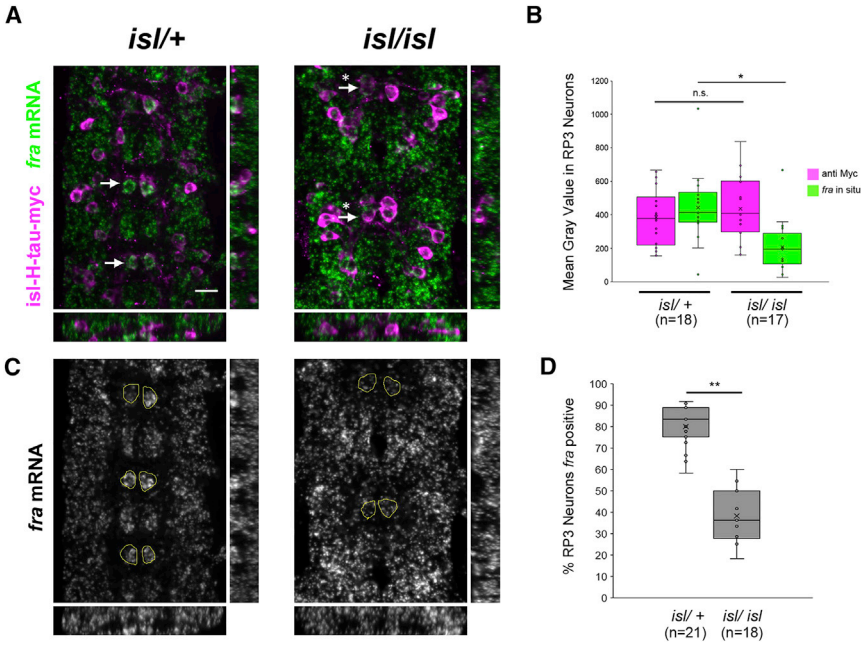

Figure 1. *Isl* Is Required for *fra* Expression in RP3 Motor Neurons

(A and C) Fluorescent in situ hybridization for *fra* in stage 15 embryos; anterior is up. In *isl*/+ embryos, *fra* mRNA (green) is enriched in RP3 neurons (arrows in A, circles in C), which are labeled by the *isl-H-tau-myc* transgene (magenta). *isl* mutants have reduced *fra* in RP3 motor neurons (arrows with asterisks). Scale bar, 10 μm.

(B) Box and whisker plots of the *fra* and *isl-tau-myc* pixel intensity signal in RP3 neurons. *isl* mutants have decreased *fra* signal (*$p < 0.001$, Student's t test) but no difference in *isl-tau-myc* signal. n, number of images analyzed.

(D) Box and whisker plots of the percentage of RP3 neurons positive for *fra* (see Experimental Procedures for scoring). *isl* mutants have fewer *fra*+ RP3 motor neurons compared with *isl*/+ embryos (**$p < 1 \times 10^{-5}$, Student's t test). n, number of embryos.

In (B) and (D), the mean is indicated by ×. Inner points and outlier points are shown. An exclusive median method was used to calculate quartiles. *isl*/+ denotes tup^{isl}/*CyO,Wgβg* or *Df(2L)Exel7072/CyO,Wgβg*. *isl/isl* denotes tup^{isl}/ *Df(2L)Exel7072*. Similar results were observed with a different *isl* allelic combination (data not shown).

See also Figure S1.

neurons (Santiago et al., 2014). Here we describe a parallel pathway by which Isl regulates *fra* expression in the same neurons and demonstrate that this pathway is important for muscle target selection. We also characterize a requirement for both *isl* and *fra* in regulating the medio-lateral position of RP3 dendrites and show that the dendrite targeting defects in *isl* mutants can be rescued by cell-type-specific overexpression of Fra. These results provide an example of how a single transcription factor contributes to neural map formation by coordinately regulating the guidance of axons to their peripheral targets, and of dendrites to their positions in the central nervous system, through its effect on a single downstream effector.

RESULTS

Isl Is Required for *fra* Expression in RP Motor Neurons

The RP3 motor neurons innervate the NetrinB-expressing muscles 6 and 7 and are enriched for *fra* mRNA during the late stages of embryonic development, and it was reported previously that, in the absence of *fra* or Netrin, there are significant defects in the innervation of muscles 6 and 7 (Kolodziej et al., 1996; Labrador et al., 2005; Mitchell et al., 1996). This phenotype is also detected in the absence of *hb9/exex* or *isl/tailup*, two transcription factors expressed in RP3 as well as in other ventrally projecting motor neurons, suggesting that *hb9* or *isl* may regulate *fra* (Broihier and Skeath, 2002; Thor and Thomas, 1997). Interestingly, Hb9, Isl, and the LIM homeodomain factor Lim3 were all recently shown to bind directly to the *fra* locus in vivo, as determined by a genome-wide DNA adenine methyltransferase identification (DAM-ID) analysis performed in *Drosophila* embryos (Wolfram et al., 2014; Figure S1). However, DAM-ID results do not provide information about the functional significance of the detected binding events or about the cell types in which they occur. To determine whether Hb9, Isl, or Lim3 regulate the expression of *fra* in embryonic motor neurons, we performed in situ hybridization experiments and analyzed *fra* mRNA expression with single-cell resolution in embryos mutant for these factors (Figure 1; Figure S2). We found that only *isl* is required for *fra* expression in the RP3 motor neurons at stage 15, when RP axons have reached the ventral muscle field but have not yet selected their final targets. 80% of RP3 neurons in abdominal segments A2–A7 in *isl*/+ embryos are positive for *fra* mRNA versus 38% in *isl* mutant embryos ($p < 0.001$; Figure 1D). We also observed a significant difference in *fra* mRNA levels in RP3 neurons between *isl* mutants and heterozygotes when quantifying pixel intensity from the *fra* in situ, whereas we detect no difference in the signal of the *isl-H-tau-myc* transgene ($p < 0.01$; Figure 1B). We detect no change in the number or position of RP3 neurons in *isl* mutants, consistent with previous data demonstrating that Isl is not required for the generation or survival of *Drosophila* motor neurons (Thor and Thomas, 1997). Importantly, we did not find a requirement for either *hb9* or *lim3* in regulating *fra* mRNA expression in any RP motor neurons (Figure S2), demonstrating that *isl*'s effect on *fra* is specific and could not have been predicted simply from similarities in loss of function phenotypes or from transcription factor binding data.

We previously found that Hb9 is required for *robo2* expression in RP3 (Santiago et al., 2014). Interestingly, just as *hb9* is not required for *fra* expression in RP neurons, *isl* is not required for *robo2* expression (Figure S2). A previous study reported that *isl; hb9* double mutants have a stronger intersegmental nerve b (ISNb) phenotype than either single mutant, but muscle 6/7 innervation defects were not quantified (Broihier and Skeath, 2002). We scored motor axon guidance defects in *isl; hb9* double

mutants and found that the double mutants display significantly more muscle 6/7 innervation defects than either single mutant (38% of hemisegments with defects in *isl; hb9* double mutants compared with 20% in *isl* mutants and 17% in *hb9* mutants, $p < 0.01$ in both cases; Figure 2C). Similarly, embryos mutant for both *robo2* and *fra* have a stronger motor axon phenotype than either *robo2* or *fra* single mutants (44% in $robo2^{ex123}$, $fra^3/robo2^{ex135}$, fra^4 mutants versus 20% in fra^3/fra^4 mutants and 21% in $robo2^{ex123}/robo2^{ex33}$ mutants; $p < 0.001$ in both cases; Figure S2). Note that, because *robo2, fra* double mutants have severe defects in midline crossing, motor axon phenotypes should be interpreted with caution (Evans et al., 2015). These results show that Hb9 and Isl act in parallel to regulate distinct downstream programs in RP3 neurons, demonstrating how combinations of transcription factors result in specific cell surface receptor profiles and axon trajectories.

Restoring *fra* Expression in *isl* Mutants Rescues Ventral Muscle Innervation

To determine whether *isl* and *fra* act in the same genetic pathway during RP3 guidance, we examined embryos mutant for both genes. In *isl*-null mutants, 20% of hemisegments lack muscle 6/7 innervation, whereas *fra*-null mutants have a significantly stronger phenotype (34% of hemisegments, $p < 0.01$; Figure 2C). *isl*, *fra* double mutants do not have more muscle 6/7 innervation defects than *fra* single mutants (40%, $p = 0.2$; Figure 2C), consistent with *isl* and *fra* acting in the same pathway. If *fra* acts downstream of Isl during motor axon targeting, then we reasoned that restoring Fra expression in *isl* mutant neurons might rescue muscle 6/7 innervation. Indeed, we found that pan-neural overexpression of Fra in *isl* mutants partially but significantly rescues these defects (Figure 2D). The difference between genotypes was most noticeable when we counted hemisegments in which a growth cone stalls at the 6/7 cleft as well as those in which it fails to reach it (all embryos were scored blind to genotype; see Experimental Procedures). In *isl* mutants, a growth cone stalls at or fails to reach the 6/7 cleft in 27% of hemisegments compared with 15% of hemisegments in sibling mutants overexpressing Fra ($p = 0.003$; Figure 2D). We also analyzed the data by comparing the number of embryos with 6/7 innervation defects. In *isl* mutants, 0% of embryos have no 6/7 innervation defects in A2–A6, 44% have one defect, and 56% have two or more defects ($n = 16$ embryos). In contrast, in *isl* mutants overexpressing Fra, 29% of embryos have no innervation defects, 29% have one defect, and 41% have two or more defects ($n = 24$ embryos, $p = 0.03$ by Fisher's exact test when comparing the number of embryos with no defects). The incomplete rescue could be due to differences in the timing or levels of *GAL4/UAS*-mediated expression of Fra compared with its endogenous regulation or could indicate that Isl regulates additional downstream effectors important in this process. Nevertheless, these data strongly suggest that Fra is an essential downstream effector of Isl during the guidance of the RP3 axon to its target muscles (Figure 2E).

Overexpression of Isl in Ipsilateral Neurons Induces *fra* Expression and *fra*-Dependent Midline Crossing

To further investigate the relationship between *isl* and *fra*, we tested whether ectopic expression of *isl* is sufficient to induce *fra* expression. For these experiments, we used the apterous (ap) neurons, a subset of interneurons whose axons form a single fascicle on either side of the midline that are labeled by *ap-Gal4* (Lundgren et al., 1995). The ap neurons express low levels of *fra* (see below), do not express *isl* (Thor and Thomas, 1997; data not shown), and do not cross the midline. Fra overexpression causes ectopic midline crossing of ap axons (Neuhaus-Follini and Bashaw, 2015; O'Donnell and Bashaw, 2013). We found that overexpression of Isl with *ap-Gal4* produces high levels of midline crossing, phenocopying the effect of Fra overexpression (Figures 2F and 2H). In stage 17 control embryos, ap axons cross the midline in 12% of segments, whereas in embryos overexpressing *UAS-Isl* with *ap-Gal4*, ap axons cross the midline in 60% of segments (Figure 2H). This phenotype is dose-dependent because embryos with two copies of an *UAS-Isl* insertion display significantly more ectopic midline crossing than embryos with one insert (84%, $p < 0.001$, data not shown).

To determine whether Isl overexpression results in *fra* induction, we analyzed the expression of *fra* mRNA in situ in ap neurons (Figure 2G). We found that, in stage 15 wild-type embryos, a low percentage of ap neurons express *fra* (25% of ventral ap clusters were *fra*+). In contrast, in embryos overexpressing *isl* from two *UAS-Isl* inserts, 37% of the ventral ap clusters were *fra*+ ($p < 0.01$ compared with controls) (Figure 2G). To test whether the ectopic crossing phenotype depends on *fra* function, we overexpressed Isl in embryos homozygous for a null allele of *fra*. Strikingly, removing *fra* completely suppresses the crossing phenotype, indicating that *fra* is required for Isl to produce its gain-of-function effect (15% of segments with ap midline crossing in fra^3/fra^3 embryos overexpressing *UAS-Isl*, $p < 0.0001$ compared with 1× GOF (gain of function) in controls, not significant (n.s.) compared with fra^3/fra^3; Figure 2H). Although we cannot rule out that Isl affects the expression of other genes in the Fra pathway to cause midline crossing, these results demonstrate that ectopically expressing Isl causes an increase in *fra* expression and a *fra*-dependent axon guidance phenotype and suggest that the functional relationship between *isl* and *fra* may be used in multiple contexts.

Isl Is Not Required for Early *fra* Expression or for RP Axon Midline Crossing

Fra mutants have defects in RP axon midline crossing, as shown by retrograde labeling of single motor neurons (Furrer et al., 2003). In addition, Netrin-Fra signaling controls the medio-lateral position of dendrites in several groups of motor neurons (Mauss et al., 2009). Therefore, we asked whether *isl* regulates midline crossing or RP3 dendrite development through *fra*. We used a genetic strategy to label single motor neurons by mosaic expression of a membrane-tethered GFP transgene under the control of *lim3b-GAL4*, which labels RP motor neurons, sensory neurons, and several other motor and interneuron populations (Certel and Thor, 2004). We identified RP3 neurons by the stereotyped position of the RP3 cell body and by the targeting of its axon to muscles 6 and 7. Because of the axon targeting defects observed in *isl* and *fra* mutants, we relied on cell body position to identify RP3 neurons in mutants. By this approach, we detect significant midline crossing defects in RP3 axons in *fra* mutants, as reported previously (18 of 23 axons fail to cross the midline in

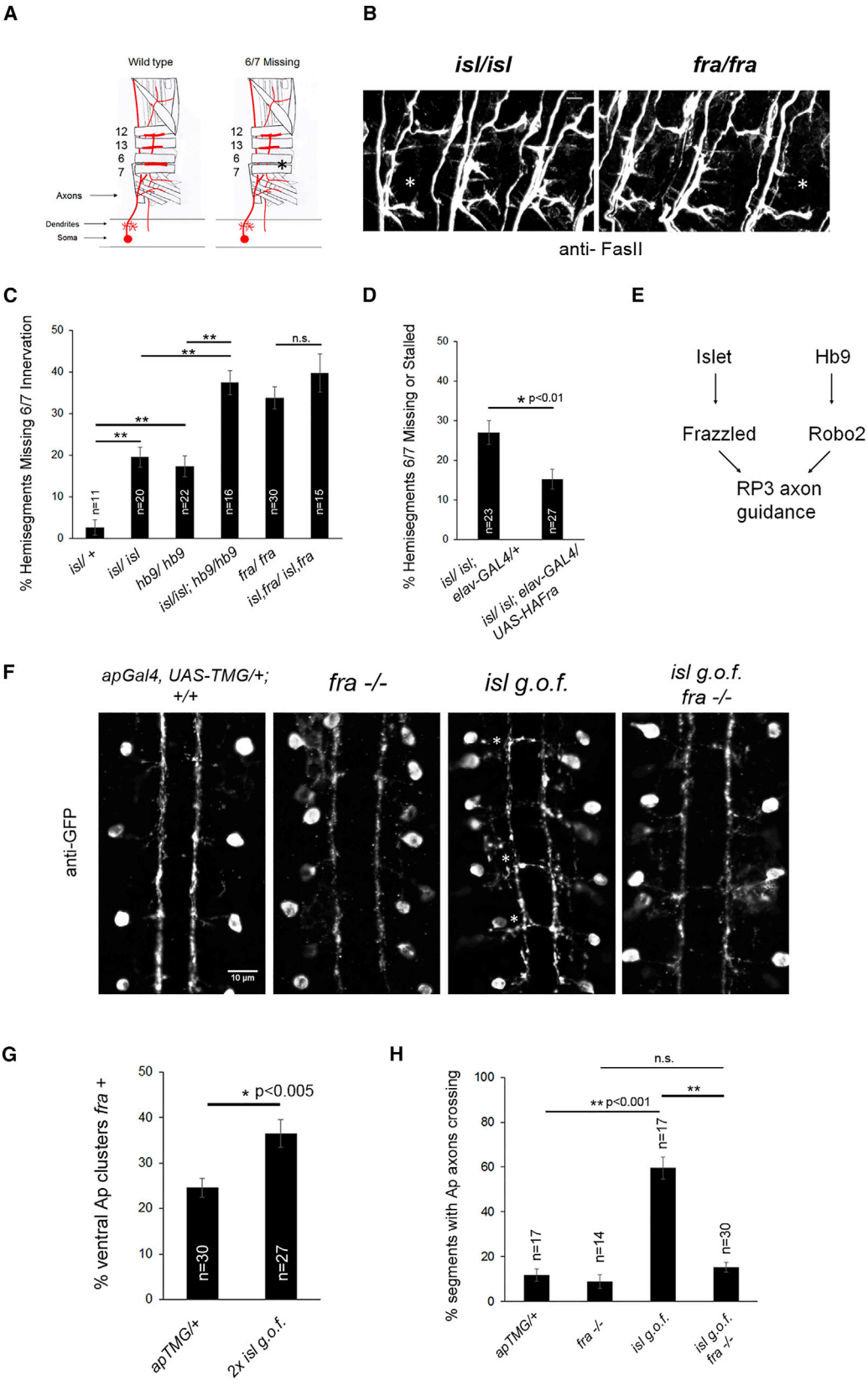

(legend on next page)

fra/fra versus 0/16 axons in *fra/+*). To our surprise, however, we observed no defects in RP axon midline crossing in *isl* mutants (33 of 33 RP3 axons cross the midline in *isl/isl*).

Isl and *fra* expression both initiate earlier than stage 13, the time at which RP axons cross the midline (Broadie and Bate, 1993; Thor and Thomas, 1997). Therefore, we examined whether *isl* is required for *fra* expression during the early stages of commissural axon guidance. Interestingly, we found that *isl* is not required for *fra* expression at stage 13 in any of the ventrally projecting RPs (Figure S3). In contrast, in stage 15 *isl* mutant embryos from the same collection, we observed a decrease in *fra* expression in RP1 and RP3 (Figures 1 and 6). The temporal pattern of *fra* expression in RP motor neurons is dynamic, so that a larger proportion of RP1 and RP3 neurons express *fra* mRNA during late embryogenesis than during the stages of midline crossing. We detect a requirement for *isl* in regulating *fra* in RP1 and RP3 as early as stage 14, when the RP motor axons have exited the CNS (Figure S3). Taken together, these results suggest that *isl* is not essential for early *fra* expression but required for *fra* expression during the late stages of motor neuron differentiation. The stages at which we detect a requirement for *isl* in regulating *fra* correspond to when RP3 axons are exploring their ventral muscle targets, consistent with a model in which Isl instructs the final stages of RP3 axon targeting through Fra.

A Difference in Dendritic Targeting between RP3 and RP5 Neurons Correlates with a Difference in *fra* Expression

Another essential feature of *Drosophila* larval motor neurons that is established late in embryogenesis is the morphogenesis and targeting of their dendrites in the ventral nerve cord. Motor neuron dendrites begin to form as extensions off the primary neurite at stage 15 (Kim and Chiba, 2004), a stage when we detect a requirement for *isl* in regulating *fra*. By early stage 17 (15 hr after egg laying, AEL), RP3 has assumed its stereotyped morphology, consisting of a small ipsilateral projection extending from the soma and a large dendritic arbor forming off the contralateral primary neurite (Mauss et al., 2009).

We used the FLP-out genetic labeling strategy to visualize individual late-stage RP motor neurons and analyze their dendrites. We focused on the large contralateral arbor of the RP motor neurons that spans one side of the nerve cord in wild-type embryos and forms branches that extend into several mediolateral zones (Mauss et al., 2009). Analyses using *isl-tau-myc* and *lim3a-tau-myc* transgenes confirmed that the RP cell bodies retain their stereotyped positions in *isl* mutants and that the relative dorsal-ventral positions of RPs 1/4, 3, and 5 are preserved, allowing us to identify distinct classes of RP motor neurons (Landgraf et al., 1997; data not shown).

We found that most RP3 neurons in late-stage *isl/+* embryos neurons form contralateral dendritic arbors that send projections into the zone between the medial FasII+ axon pathways and the intermediate FasII+ pathways, hereafter referred to as the ''intermediate zone,'' consistent with previously published images of RP3 neurons from wild-type embryos (89%, n = 18; Figure 3A; Movie S1). Interestingly, the dendritic morphology of RP3 was distinct from that of a related neuron, RP5, that also expresses Isl and Lim3b-Gal4 and that can be unambiguously identified in both wild-type and mutant embryos because its cell body is found in a more ventral position than the other RP neurons (Landgraf et al., 1997; Movie S2). In wild-type embryos, the RP5 axon targets muscles 12 and 13 (VL1 and VL2) as well as other ventral muscles (Landgraf et al., 1997; Mauss et al., 2009). Most RP5 neurons in *isl/+* embryos exclusively target their dendrites to the lateral zone of the neuropile (80%, n = 20; Figure 3A). Furthermore, the difference we observe in the dendritic targeting of RP3 and RP5 neurons correlates with a difference in *fra* expression. Although *fra* expression in RP3 and RP5 neurons in control embryos is comparable when RP axons are crossing the midline (Figure S3), by stage 15, significantly fewer RP5 than RP3 neurons express *fra* (Figure 3B). Interestingly, *isl* is not required for the low levels of *fra* expression in late-stage RP5 neurons, in contrast to its role in promoting high levels of *fra* in late-stage RP3 neurons (Figure 3B).

Finally, we monitored endogenous Netrin expression in late-stage nerve cords using a Myc-tagged *NetB* knockin allele (Brankatschk and Dickson, 2006) and detected significant

Figure 2. Isl Acts through *fra* to Regulate RP3 Motor Axon Guidance, and Isl Overexpression in Interneurons Induces *fra* Expression and a Midline-Crossing Phenotype

(A) Schematic of two hemisegments; dorsal is up and anterior is left. The asterisk indicates the absence of muscle 6/7 innervation by RP3.

(B) *isl* or *fra* mutant embryos stained for FasII, which labels all motor axons. Asterisks indicate an absence of muscle 6/7 innervation.

(C and D) Quantification of muscle 6/7 innervation defects. (C) *isl; hb9* double mutants have an additive phenotype compared with the single mutants (**$p < 0.001$, Student's t test), whereas *isl, fra* double mutant embryos are not enhanced relative to *fra* mutants ($p = 0.2$, Student's t test). (D) *isl* mutants overexpressing Fra panneurally have fewer defects than sibling mutants (*$p < 0.01$, Student's t test).

(E) Model for how Isl and Hb9 regulate RP3 axon guidance (see also Santiago et al., 2014).

(F) Stage 17 embryos in which the ap neurons are labeled with ap^{Gal4} > *UAS-TauMycGFP*. Isl overexpression causes ectopic midline crossing (asterisks), which is suppressed when Isl is overexpressed in *fra* mutants.

(G) Quantification of *fra*+ ventral ap neurons in wild-type embryos and embryos overexpressing Isl, following in situ hybridization for *fra* mRNA. Overexpression of *UAS-Isl* causes upregulation of *fra* in ventral ap neurons (*$p < 0.005$, Student's t test).

(H) Quantification of ap axon midline crossing. Isl gain of function causes ectopic crossing (**$p < 0.001$, Student's t test) but not when Isl is overexpressed in *fra*-null mutants.

In (C), *isl/+* denotes *Df(2L)Exel7072/ CyO,Wgβg*. *isl/isl* denotes *Df(2L)Exel7072/ Df(2L)Exel7072*. *hb9/hb9* denotes $hb9^{kk30}/hb9^{ad121}$. *isl/isl; hb9/hb9* denotes *Df(2L)Exel7072/ Df(2L)Exel7072; *$hb9^{kk30}/hb9^{ad121}$. *fra/fra* denotes fra^3/fra^3. *isl,fra/isl,fra* denotes *Df(2L)Exel7072,*fra^3*/ Df(2L)Exel7072,*fra^3. In (D), *isl/isl* denotes tup^{isl}/*Df(2L)Exel7072*. In (F)–(H), *fra/fra* denotes $fra^3,ap^{Gal4}/fra^3$*,UAS-TMG*. *isl g.o.f.* denotes ap^{Gal4}*,UAS-TMG/+; UAS-Isl5xMyc/+*. *isl g.o.f. in fra −/−* denotes $fra^3,ap^{Gal4}/fra^3$*,UAS-TMG; UAS-Isl5xMyc/+*. *2x isl g.o.f.* denotes ap^{Gal4}*, UAS-TMG/+; UAS-Isl5xMyc/UAS-Isl5xMyc*. n, number of embryos. Scale bars, 10 μm. Error bars indicate SEM. See also Figures S2 and S3.

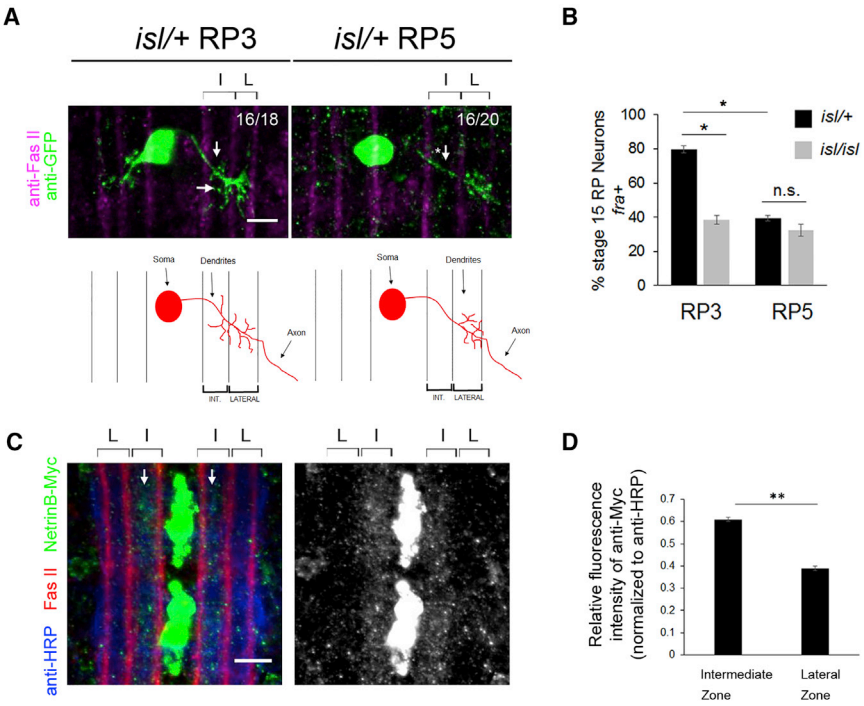

Figure 3. A Difference in the Dendrite Positions of Two Classes of Motor Neurons Correlates with a Difference in *fra* Expression, and Netrin Is Enriched in the Intermediate Zone

(A) Top: single-labeled neurons from stage 17 *isl*/+ embryos. RP3 and RP5 neurons are labeled with anti-GFP (green); FasII+ axons are stained (magenta). The intermediate zone is innervated by RP3 dendrites (arrows) but not by RP5 dendrites (arrow with asterisk). Bottom: cartoons of RP motor neurons; FasII+ axon pathways are shown in black. The intermediate zone is the space between the medial and FasII+ axon tracts.

(B) Quantification of the percentage of RP3 or RP5 neurons positive for *fra* mRNA in *isl*/+ and *isl*/*isl* embryos at stage 15. More RP3 neurons than RP5 neurons express *fra* in *isl*/+ embryos (*p < 0.001). *isl* is not required for *fra* expression in RP5 (p = 0.26). n, number of embryos.

(C) Stage 17 embryo expressing myc-tagged NetrinB (green) from its endogenous locus, stained with anti-Fas II (red) and anti-HRP (blue). NetrinB is highly expressed in midline glia and is enriched on axons in the intermediate zone.

(D) Quantification of the fluorescence intensity of NetrinB-myc staining, normalized to anti-HRP. There is increased anti-Myc signal in the intermediate zone compared with the lateral zone (**p < 0.0001, Student's t test).

Error bars indicate SEM. Scale bars, 5 μm. *isl*/+ denotes tup^{isl}/*CyO,Wgβg* or *Df(2L)Exel7072/ CyO,Wgβg*. *isl*/*isl* denotes tup^{isl}/ *Df(2L)Exel7072*. See also Movies S1 and S2.

enrichment of Netrin protein in the area between the intermediate and medial FasII+ axon bundles (Figures 3C and 3D). This area corresponds to the zone where we detect contralateral dendritic projections from RP3 neurons, suggesting that high levels of Fra in RP3 may instruct the formation of dendritic arbors in this region in response to Netrin.

Isl and *fra* Regulate the Targeting of RP3 Motor Neuron Dendrites in the CNS

We next analyzed RP motor neuron dendrites in *isl* mutant embryos to determine whether Isl regulates dendritic position or morphogenesis through Fra or other effectors. We did not observe a significant difference in the morphology or medio-lateral position of RP5 dendrites between heterozygous and mutant embryos (data not shown). In striking contrast, many RP3 neurons in *isl* mutants fail to extend contralateral dendrites into the intermediate zone (48%, n = 33, p = 0.01 compared with *isl*/+ embryos, Fisher's exact test; Figures 4A and 4B). Instead, the dendrites of these RP3 neurons remain fasciculated with the intermediate FasII+ axon pathways and do not send medial extensions toward the midline (Figure 4A). To more quantitatively measure medio-lateral position and to address the possibility that defects in targeting are secondary to defects in outgrowth, we traced RP3 neurons using Imaris software and measured total contralateral dendrite lengths and the total number of dendrite tips (Figures 4C–4F; see Figure S4 for additional examples of dendritic traces and Movies S3 and S4 for examples of z stacks that were used for tracing). We also measured the total length of contralateral dendrites in the intermediate zone of the neuropile, defined as the area between the medial FasII+ and the intermediate FasII+ axon pathways (Figures 4C and 4D). Although RP3 neurons displayed increased variability in the size of their dendritic arbors in *isl* mutants, there was no significant difference in the total length or tip number of RP3 dendrites between *isl* mutants and heterozygotes, suggesting that targeting defects in *isl* mutants are not likely due to reduced outgrowth (Figures 4E and 4F). However, the ratio of RP3 dendrites in the intermediate zone over total RP3 dendrite length was significantly reduced in *isl* mutants, confirming that *isl* mutant RP3 dendrites are shifted laterally relative to controls (p = 0.01; Figures 4C and 4D).

We next analyzed the dendrites of RP3 neurons in *fra*/+ and *fra* mutant embryos (Figure 5). As with *isl* mutants, we relied upon cell body position to identify RP3 neurons and excluded neurons with ambiguous positions (Supplemental Experimental Procedures). In *fra* mutant RP3 neurons whose axons fail to cross the midline, a single dendritic arbor forms off the ipsilateral primary neurite, and we traced this arbor. We observed a significant lateral shift in the position of RP3 dendrites in *fra* mutants both by scoring for the presence of dendrites in the intermediate zone and by quantitative analysis of the dendrites of traced neurons (Figures 5B and 5C). The lateral shift in *fra* mutants was more pronounced than in *isl* mutants, consistent with our observation that some RP3 neurons retain *fra* expression in the absence of *isl* (Figure 1). Of note, the lateral shift phenotype did not correlate with whether the RP3 axon had crossed the midline because we detected it at similar frequencies in both contralateral and ipsilateral arbors (Figure 5A). Curiously, several RP3 contralateral dendritic arbors appeared reduced in size in

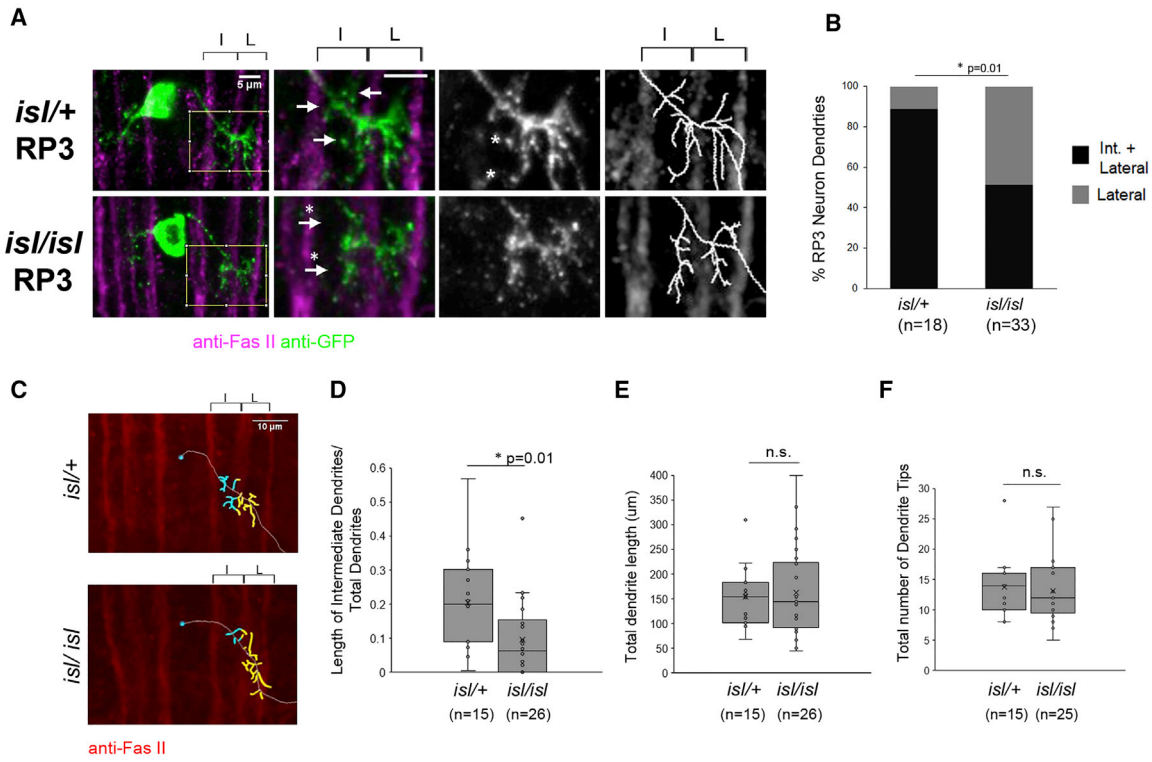

G

	Dendrites target correct zone Axon to 6/7	Shifted Dendrites Axon to 6/7	Dendrites target correct zone Axon misprojects	Shifted Dendrites Axon misprojects
isl/+	12	2	0	0
isl/isl	9	9	3	5

Figure 4. *Isl* Regulates the Medio-lateral Targeting of RP3 Dendrites in the CNS

(A) RP3 neurons from stage 17 embryos of the indicated genotypes are labeled with anti-GFP (green); FasII+ axons are stained (magenta). Arrows point to the intermediate zone; arrows with asterisks point to dendrites that fail to target the intermediate zone. Higher-magnification panels of the selected areas are shown. Asterisks indicate background fluorescence from a cell in another plane. Right: contralateral dendrites were traced on Imaris; skeletons of traces are shown against FasII+ axons.

(B) Percentage of RP3 neurons that target their contralateral dendrites to intermediate and lateral regions of the nerve cord. Fewer RP3 neurons extend dendrites into the intermediate zone in *isl/isl* embryos (*$p < 0.05$, Fisher's exact test).

(C) Examples of dendrite traces in *isl/+* and *isl/isl* embryos in which intermediate and lateral dendrites are color-coded in cyan and yellow, respectively. FasII+ axons are shown in red.

(D) Box and whisker plots of the length of RP3 contralateral dendrites in the intermediate zone divided by the total length of RP3 contralateral dendrites. *isl/isl* neurons have a reduction in the fraction of dendrites in the intermediate zone ($p = 0.01$, Student's t test).

(E) Box and whisker plots of the total length of contralateral RP3 dendrites. There is no significant difference between *isl/+* and *isl/isl* neurons ($p = 0.75$).

(F) Box and whisker plots of the number of contralateral dendrite tip endings. There is no significant difference between *isl/+* and *isl/isl* embryos ($p = 0.67$).

(G) Summary of the frequency of axon and dendrite defects detected in *isl/+* and *isl/isl* RP3 neurons. n, number of neurons.

In (D)–(F), the mean is indicated by ×. Inner points and outlier points are displayed. An exclusive median method was used to calculate quartiles. *isl/+* denotes *tup^{isl}, lim3b-Gal4/CyO,elavβg*. *isl/isl* denotes *tup^{isl}, lim3b-Gal4/Df(2L)Exel7072*. Scale bars, 5 μm. See also Figure S4 and Movies S3 and S4.

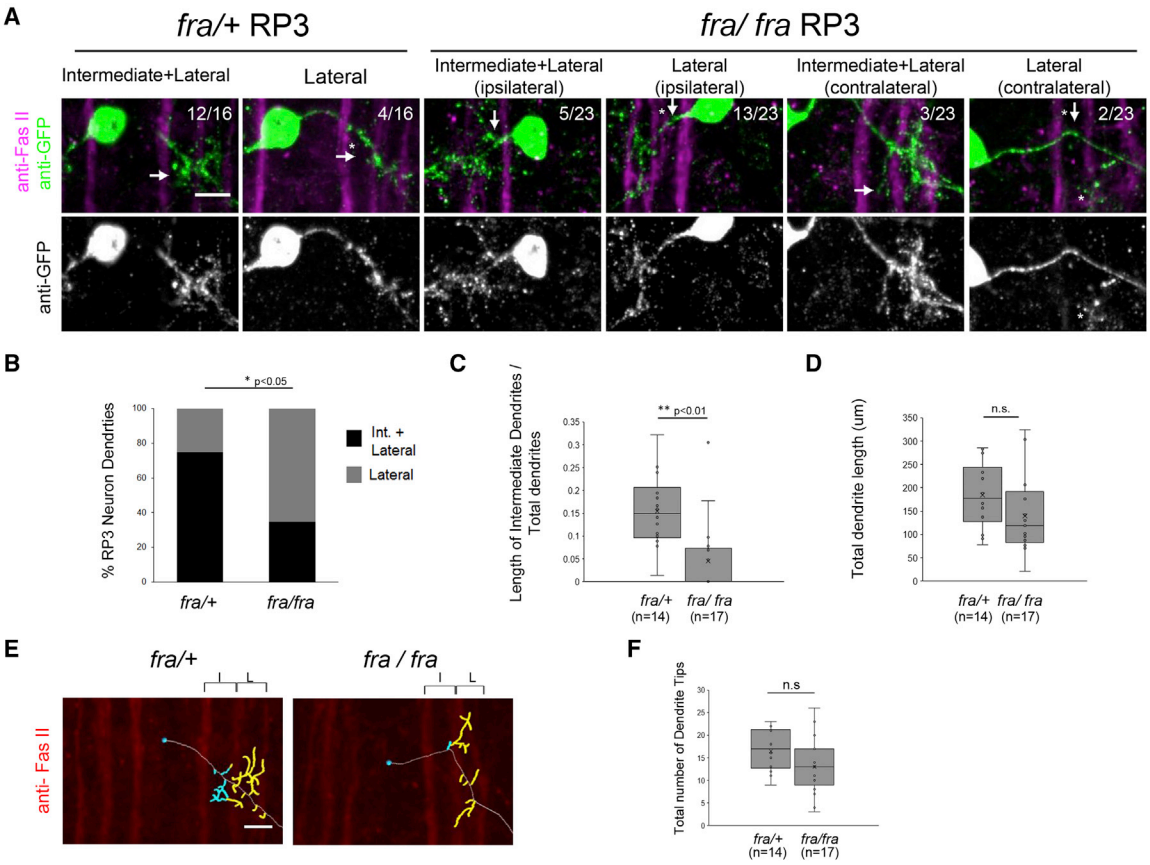

Figure 5. *fra* Regulates the Medio-lateral Targeting of RP3 Dendrites

(A) RP3 neurons from stage 17 embryos stained with anti-GFP (green); FasII+ axons are shown in magenta. Many dendritic arbors fail to target the intermediate zone in *fra/fra* mutants; this phenotype does not correlate with defects in midline crossing. Arrows point to dendrites in the intermediate zone; arrows with asterisks point to laterally shifted dendrites. Isolated asterisks indicate GFP fluorescence from another cell.

(B) Percentage of RP3 neurons targeting their dendrites to intermediate and lateral regions. Significantly fewer RP3 neurons extend dendrites into the intermediate zone in *fra/fra* embryos (*$p < 0.05$, Fisher's exact test).

(C) Box and whisker plots of the length of RP3 dendrites in the intermediate zone divided by the total length of RP3 dendrites in *fra*/+ and *fra/fra* neurons. There is a significant reduction in the fraction of intermediate dendrites in *fra* mutants (**$p < 0.01$, Student's t test).

(D) Box and whisker plots of total dendrite lengths; there is no significant change between *fra*/+ embryos and *fra/fra* mutants ($p = 0.11$).

(E) RP3 dendrite skeletons in which intermediate and lateral dendrites are color-coded in cyan and yellow, respectively.

(F) Box and whisker plot of total dendrite tip numbers; there is no significant change between *fra*/+ embryos and *fra* mutants ($p = 0.09$).

In (C), (D), and (F), the mean is indicated by ×. Inner points and outlier points are displayed. An exclusive median method was used to calculate quartiles. n, number of neurons. *fra*/+ denotes *fra*^{3}, *lim3b-Gal4/CyO,elavβg*. *fra/fra* denotes *fra*^{3}, *lim3b-Gal4/fra*^{3}. Scale bars, 5 μm. See also Figure S4.

fra mutants (Figure 5A, sixth panel), whereas this phenotype was not seen in control embryos. However, as in *isl* mutants, there was no significant change in the total dendrite length or tip number in *fra* mutants compared with their sibling controls, although there was increased variability in the sizes of dendritic arbors in the mutants (Figures 5D and 5F). These findings are consistent with previous reports that Netrin-Fra signaling does not play a major role in regulating the outgrowth of motor neuron dendrites in the nerve cord (Brierley et al., 2009; Mauss et al., 2009).

Axon and Dendrite Targeting Defects Are Not Correlated in Individual RP3 Neurons

Our single-cell labeling method allows us to precisely describe the axon targeting defects in *isl* and *fra* mutants and determine whether they correlate with defects in dendrite position. Axon and dendrite targeting occur at approximately the same developmental stage, and there is no evidence that one process depends on the other (Kim and Chiba 2004; Landgraf et al., 2003). Importantly, previous studies using retrograde labeling of motor neurons in mutant embryos were not able to address this question because they relied upon motor axons reaching the correct muscles to be visualized (Mauss et al., 2009).

To determine whether defects in dendrite position correlate with defects in axon targeting, we scored both phenotypes in single labeled RP3 neurons in embryos with muscles fully preserved following dissection. All of the RP3 axons that we were able to score in *isl* heterozygous embryos innervated the muscle 6/7 cleft (n = 14; Figure 4G). In contrast, 18 of 26 *isl* mutant RP3

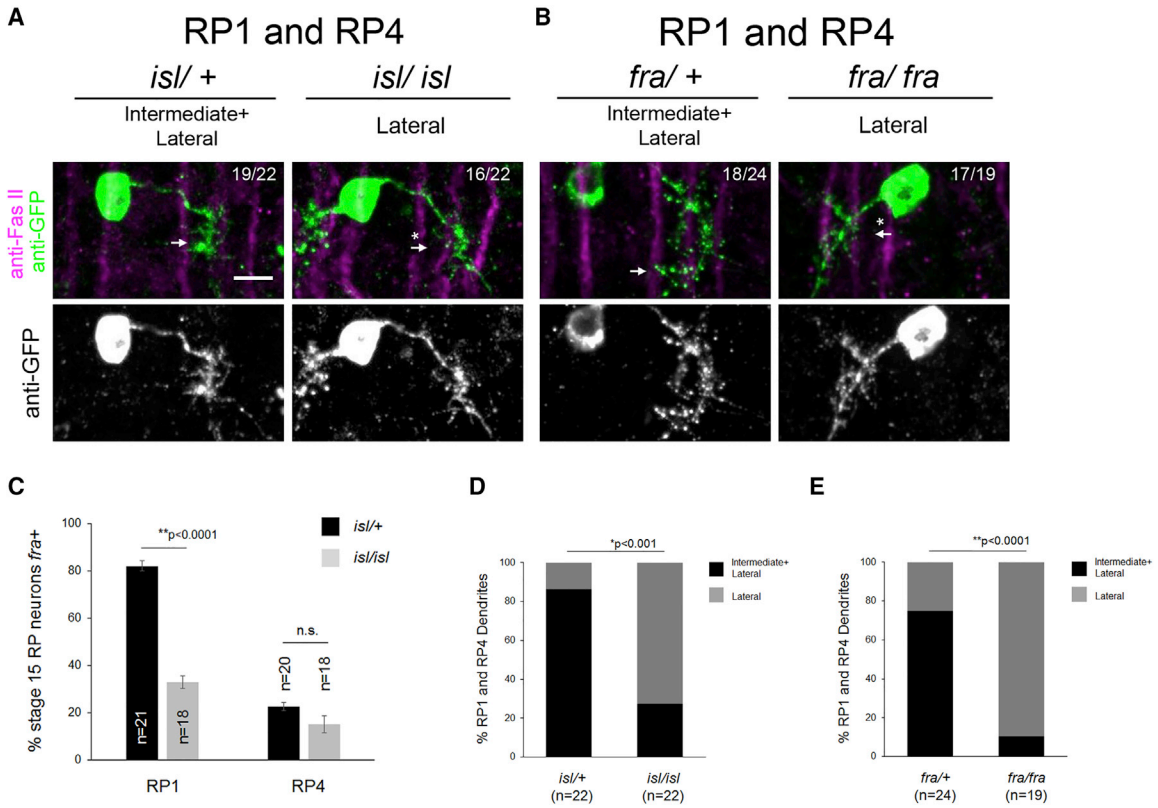

Figure 6. RP1 and RP4 Dendrites Are Shifted Laterally in *isl* and *fra* Mutants, and RP1 Neurons Require *isl* for *fra* Expression

(A and B) RP1 and RP4 neurons from stage 17 embryos stained with anti-GFP (green). FasII+ axons are shown in magenta. The majority of RP1/RP4 neurons target their dendrites to the intermediate and lateral regions of the nerve cord in *isl*/+ embryos (A) and in *fra*/+ embryos (B) (arrows), whereas many fail to target the intermediate zone in *isl*/*isl* (A) or *fra*/*fra* mutants (B) (arrows with asterisks).

(C) Percentage of RP neurons positive for *fra* mRNA at stage 15 in *isl*/+ and *isl*/*isl* embryos. In control embryos, fewer RP4 neurons than RP1 neurons express *fra*. *isl* is not required for *fra* expression in RP4 neurons ($p = 0.2$), but is required for *fra* expression in RP1 neurons (**$p < 0.0001$, Student's t test).

(D and E) Percentage of RP1 and RP4 neurons that target their dendrites to intermediate or lateral regions. *isl* mutants (D) and *fra* (E) mutants have fewer RP1 and RP4 dendritic arbors in the intermediate zone compared with controls (*$p < 0.001$, **$p < 0.0001$, Fisher's exact test).

In (C), error bars indicate SEM. n, number of embryos. In (D) and (E), n, number of neurons. *isl*/+ denotes tup^{isl}/*CyO,Wg*β*g* or *Df(2L)Exel7072*/ *CyO,Wg*β*g*. *isl*/*isl* denotes tup^{isl}/ *Df(2L)Exel7072*. *fra*/+ denotes fra^3, *lim3b-Gal4*/*CyO,elav*β*g*. *fra*/*fra* denotes fra^3, *lim3b-Gal4*/fra^3. Scale bars, 5 μm.

axons innervated muscles 6/7, and eight stalled at the 6/7 cleft or earlier along RP3's trajectory or bypassed the choice point (31% have defects, n = 26; Figure 5G). In *fra* mutant embryos, 10 of 22 RP3 neurons failed to innervate the muscle 6/7 cleft and stalled at or bypassed the choice point (45% have defects, data not shown). This phenotype is stronger than the frequency at which we detect a complete loss of muscle 6/7 innervation in *isl* or *fra* mutants by scoring with anti-FasII (Figure 2). To determine whether this enhancement was due to the heat shock (H.S.) step that is required for genetic labeling, we scored defects using anti-FasII in embryos heat-shocked for either 5 min or 1 hr (Experimental Procedures) and found that the 1-hr H.S. mildly enhances muscle innervation defects in *isl* mutants (to 30.4%) whereas a 5-min H.S. does not (to 24.7%, data not shown). Importantly, the two H.S. protocols did not result in any difference in the frequency of dendrite targeting defects observed in *isl* mutants because 7 of 17 RP3 dendrites in *isl* mutants are shifted laterally in embryos treated with 1-hr H.S, and 9 of 16 dendrites are shifted after 5-min H.S (data not shown).

To our surprise, we did not detect a correlation between axon and dendrite defects in *isl* mutants (Figure 4G). Although 5 of 26 RP3 neurons displayed defects in both axons and dendrites in *isl* mutants, 12 of 26 neurons showed defects in one process but not the other (Figure 4G). A similar analysis in *fra* mutants revealed that 8 of 22 RP3 neurons displayed defects in both muscle 6/7 innervation and dendrite position, whereas 8 of 22 displayed normal targeting in one process but not the other (data not shown). These data suggest that axon and dendrite targeting can occur independently within an individual RP3 neuron and that the central targeting defects we observe in *isl* mutants are not likely to be secondary to defects in muscle innervation.

Isl and *fra* Regulate the Targeting of RP1 and RP4 Motor Neuron Dendrites

We next asked whether *isl* and *fra* regulate dendrite development in other classes of motor neurons. RP1 and RP4 also express *isl*, *fra*, and *lim3b-Gal4*. We detect a requirement for *isl* in regulating *fra* expression in RP1, but not in RP4, at stage 15 (Figure 6C).

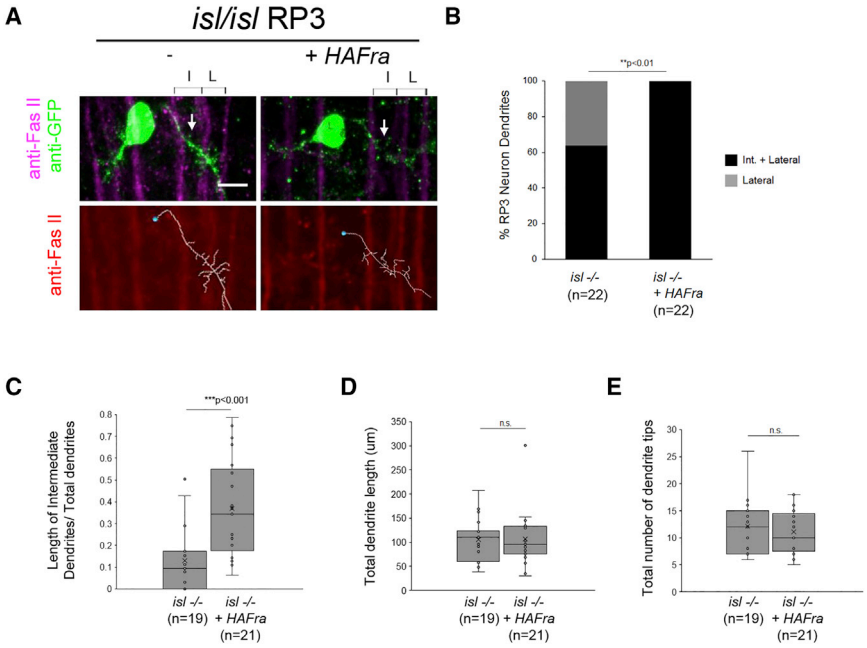

Figure 7. Cell-Type-Specific Overexpression of Fra in *isl* RP3 Motor Neurons Rescues the Position of Their Dendrites

(A) RP3 neurons from stage 17 embryos. Top: RP3 neurons are stained with anti-GFP (green), and FasII+ axons (magenta) are stained. Arrows point to dendrites in the intermediate zone. Bottom: contralateral dendrites were traced on Imaris; traces are shown as skeletons (white) against FasII+ axons (red).

(B) Percentage of RP3 neurons that target their dendrites to intermediate and lateral regions. All RP3 dendrites are present in the intermediate zone in *isl/isl* embryos overexpressing Fra, whereas many dendrites in sibling *isl/isl* embryos lacking the transgene fail to target the intermediate zone (**$p < 0.01$, Fisher's exact test).

(C) Box and whisker plots of the lengths of RP3 contralateral dendrites in the intermediate zone divided by the total length of RP3 contralateral dendrites. *isl/isl* neurons overexpressing Fra display an increase in the fraction of intermediate dendrites compared with *isl/isl* neurons (***$p < 0.001$, Student's t test).

(D) Box and whisker plots of total lengths of contralateral RP3 dendrites. There is no significant difference between *isl/isl* neurons and *isl/isl* neurons overexpressing Fra ($p = 0.95$).

(E) Box and whisker plots of the total number of contralateral dendrite tip endings. There is no significant difference between *isl/isl* embryos and *isl/isl* embryos overexpressing Fra ($p = 0.5$). n, number of neurons.

In (C)–(E), the mean is indicated by ×. Inner points and outlier points are displayed. An exclusive median method was used to calculate quartiles. *isl/isl* denotes tup^{isl}, *lim3b-Gal4/Df(2L)Exel7072*. *isl/isl+ HAFra* denotes tup^{isl}, *lim3b-Gal4/Df(2L)Exel7072; UAS-HAFra 86fb/+*. Scale bar, 5 μm.

Interestingly, most RP1 neurons, like RP3 neurons, retain high levels of *fra* at this stage, whereas few RP4 neurons express *fra* in late-stage control embryos (Figure 6C). Previous descriptions of RP1 and RP4 neurons indicate that they form contralateral dendritic arbors of distinct morphologies; RP1's dendritic arbor is taller and found more medially (Mauss et al., 2009). However, because the axons of RP1 and RP4 target adjacent muscles external to muscles 6 and 13, and their cell bodies are found close to the midline at a similar dorsal-ventral position, we could not unambiguously distinguish between them in our single-cell labeling experiments. Nevertheless, when we scored RP1 and RP4 neurons together, we observed a significant lateral shift in the position of RP1 and RP4 dendrites in *isl* mutants compared with heterozygous siblings: 3 of 22 RP1 and RP4 dendritic arbors were excluded from the intermediate zone in *isl* heterozygous embryos (14%) compared with 16 of 22 in mutant embryos (73%; $p = 0.0002$, Fisher's exact test; Figures 6A and 6D). We detected a similar phenotype in RP1 and RP4 dendrites in *fra* mutants. Specifically, 6 of 24 RP1 and RP4 dendritic arbors were excluded from the intermediate zone in heterozygotes (25%) compared with 17/19 in *fra* mutants (93%; $p < 0.0001$, Fisher's exact test; Figures 6B and 6E). Although additional work will be necessary to determine whether the defects in dendrite position that we detect in RP1 and RP4 neurons in *isl* mutants correlate with changes in *fra* expression, these data demonstrate that Isl is required for high levels of *fra* expression in at least two classes of motor neurons (RP1 and RP3), both of which require *isl* and *fra* for dendritic targeting.

Isl Regulates Dendrite Development in RP3 Neurons through *fra*

To directly test whether *isl* regulates RP3 dendrite position through its effect on *fra* expression, we overexpressed a *UAS-HA-Fra* transgene using *lim3b-GAL4* in *isl* mutants and used the *hsFLP* technique to sparsely label RP motor neurons (Figure 7). Strikingly, in *isl* mutants overexpressing Fra, 0 of 21 RP3 contralateral dendritic arbors were excluded from the intermediate zone compared with 8 of 22 (36%) in sibling mutants lacking the *UAS-Fra* transgene ($p < 0.01$, Fisher's exact test; Figure 7B). To quantitatively measure dendrite position, we obtained traces of RP3 dendrites. We detected a robust rescue of the lateral shift phenotype in *isl* mutants, as measured by the length of dendrites in the intermediate zone over the total dendrite length ($p < 0.001$, Student's t test; Figure 7C). Indeed, the ratio of dendrites in the intermediate zone in rescued mutants was higher than in heterozygous controls, perhaps reflecting a gain-of-function effect caused by artificially high levels of Fra from transgenic overexpression. Importantly, Fra overexpression did not have any effect on total dendritic arbor lengths or tip numbers (Figures 7D and 7E), strongly arguing that the rescue we observe is not caused by an increase in the total size of the arbors. Although we cannot rule out that Isl regulates dendrite position in part through additional effectors, our observation that cell-type-specific overexpression of Fra in *isl* mutants rescues dendrite targeting provides compelling support for the model that *fra* acts downstream of *isl* to control RP3 dendrite morphogenesis. Together with our demonstration that *isl* directs

RP3 motor axon targeting through the regulation of *fra*, we conclude that *isl* coordinately regulates the targeting of axons in the periphery and of dendrites in the CNS through a common downstream effector.

DISCUSSION

It is well established that transcription factors play subset-specific roles in regulating neural morphogenesis, but identifying the cellular effectors that act downstream of these factors remains a major challenge, as does understanding how individual transcription factors coordinately establish multiple aspects of cell fate. In this study, we show that *isl* is required for *fra*/*DCC* expression in a subset of *Drosophila* motor neurons and that this regulatory relationship contributes to two key aspects of motor neuron morphology. Loss of function and genetic rescue experiments indicate that *fra* acts downstream of *isl* in motor neurons both during axon guidance in the periphery and dendrite targeting in the CNS. These data describe a mechanism by which a single transcription factor contributes to neural map formation by controlling the position of both the inputs and outputs of a neuron through an identified downstream effector.

A Role for a Cell-Type-Specific Transcription Factor in Controlling Myotopic Map Formation

In the vertebrate spinal cord, the position of motor neuron cell bodies correlates with the targeting of their axons in the periphery (Catela et al., 2015). This myotopic map may be established through the action of transcription factors that coordinately control cell migration and axon guidance. In particular, Lhx1 and Isl1 are expressed in limb-innervating lateral motor column (LMC) motor neurons and regulate the trajectory of their axons as well as the medio-lateral settling position of their cell bodies (Kania and Jessell, 2003; Luria et al., 2008; Palmesino et al., 2010). Lhx1 and Isl1 regulate axon guidance through EphA4 and EphB receptors, respectively, and a recent study suggests that Lhx1 regulates cell body position through a distinct effector, the Reelin signaling protein Dab-1 (Palmesino et al., 2010).

In *Drosophila*, unlike in vertebrates, the position of motor neuron cell bodies does not necessarily correlate with the targeting of their axons in the periphery because neurons that innervate adjacent muscles can be found far apart within a segment (Landgraf et al., 2003; Mauss et al., 2009). Instead, recent studies have shown that both the larval and the adult *Drosophila* nervous systems use a myotopic map in which the position of motor neuron dendrites, rather than their cell bodies, correlates with the position of their target muscles (Brierley et al., 2009; Mauss et al., 2009). This may be a conserved feature of motor systems across phyla because the dendritic patterning of at least four motor neuron pools in the spinal cord correlates with muscle target identity in the mouse (Vrieseling and Arber, 2006).

Slit-Robo, Netrin-Fra, and Sema-Plexin signaling have been shown to control motor neuron dendrite targeting in *Drosophila*, and rescue experiments suggest that these guidance receptors act cell-autonomously in this process (Brierley et al., 2009; Mauss et al., 2009; Syed et al., 2016). In addition, the initial targeting of motor neuron dendrites in the embryo is largely unaffected by manipulations that affect the position or the activity of pre-synaptic axons or the presence of muscles, suggesting that this process is likely under the control of cell-autonomous factors, although these remain unidentified (Landgraf et al., 2003; Mauss et al., 2009).

We address several key questions about how motor neuron dendrite targeting is specified in *Drosophila*. First, we show that *fra* expression in two classes of motor neurons (RP3 and RP5) correlates with the medio-lateral position of their dendrites. Previous studies suggested that different classes of motor neurons express different levels of guidance receptors to direct the position of their dendrites, but this had not been demonstrated. Second, we find that Isl, which was shown previously to regulate axon targeting in a subset-specific way, also regulates dendrite targeting. Third, we find that Isl regulates both processes through *fra*. Surprisingly, we did not detect a correlation between axon and dendrite phenotypes in *isl* mutants. The absence of a correlation suggests that the dendrite positioning defects are not secondary to defects in target selection, consistent with a previous study in which the general patterning of motor neuron dendrites was not disrupted in muscle-less embryos (Landgraf et al., 2003). However, additional experiments that disrupt axon targeting and monitor the medio-lateral position of dendrites will be necessary to confirm that the two occur independently.

Future work will also be necessary to identify additional transcription factors that specify motor neuron dendrite development. We previously identified a role for Hb9 in regulating *robo2* and *robo3* expression, but it is not known whether these receptors regulate motor neuron dendrite development (Santiago et al., 2014). We detect no change in *robo1* mRNA levels in RP3 neurons in either *hb9* or *isl* mutants (data not shown). Robo signaling could be regulated post-transcriptionally. Comm is required for midline crossing of motor neuron dendrites and may endogenously regulate their medio-lateral position (Furrer et al., 2003, 2007). The temporal pattern of *comm* expression does not support a role in dendrite targeting, however, because *comm* is not expressed in RP motor neurons at late stages of embryogenesis (Keleman et al., 2002; C.S. and G.J.B., unpublished data).

The functional consequences of dendrite targeting defects remain to be explored. It is likely that shifting the position of motor neuron dendrites alters their connectivity, but testing this hypothesis will require identifying the pre-synaptic neurons that impinge on the RPs during locomotive behavior. Forcing a shift in the position of dendrites of dorsally projecting motor neurons does not abolish their connectivity with known pre-synaptic partners but does change the number of contacts established (Couton et al., 2015). In mice, the ETS factor Pea3/Etv4 is required for the dendritic patterning of a subset of motor neurons, and electrophysiological recordings reveal changes in connectivity in *Pea3* mutant spinal cords (Vrieseling and Arber, 2006). It will be of high interest to investigate whether analogous defects are detected in *isl* or *fra* mutant embryos.

Isl Is an Essential Regulator of Multiple Features of RP3 Identity

Drosophila Isl was initially described as a subset-specific regulator of axon guidance (Thor and Thomas, 1997). More recently,

Wolfram et al. (2012) demonstrated that Isl also acts instructively to establish the electrophysiological properties of RP motor neurons through repression of the potassium ion channel Shaker. Our data show that, in addition to regulating the axonal trajectory and the electrophysiological properties of the RP3 neuron, Isl also establishes its dendritic position. Hobert (2015) has defined terminal selectors as transcription factors that coordinately regulate gene programs conferring multiple aspects of a neuron's identity, including its neurotransmitter phenotype, ion channel profile, and connectivity. Unlike the early-acting factors that function transiently to specify cell fate, terminal selectors are expressed throughout the life of an animal and are required for the maintenance of neural identity. Although there are several examples of transcription factors that act this way, it remains unclear how widespread a phenomenon it is (Allan et al., 2005; Eade et al., 2012; Flames and Hobert, 2009; Kratsios et al., 2011; Lodato et al., 2014). Does Isl fit the criteria for a terminal selector? Isl is not required for all aspects of RP3 identity because RP neurons retain expression of other motor neuron transcription factors in *isl* mutants, and their axons exit the nerve cord (Broihier and Skeath, 2002; Thor and Thomas, 1997). Future work will be necessary to determine whether Isl is required throughout larval life for the maintenance of RP3's physiological and morphological features and to what extent Isl coordinately establishes multiple features of RP neuron identity.

Hb9 and *isl* Act in Parallel to Regulate Axon Guidance through Distinct Downstream Effectors

Co-expressed transcription factors could act synergistically to regulate specific downstream programs, in parallel through completely distinct effectors, or by some combination of the two mechanisms. Indeed, examples of all of these scenarios have been described. Both in vitro and in vivo studies demonstrate that, in vertebrate spinal motor neurons, Isl1 forms a complex with Lhx3 and that the Isl1-Lhx3 complex binds to and regulates different genes than Lhx3 alone or than a complex composed of Isl1 and Phox2b, a factor expressed in hindbrain motor neurons (Cho et al., 2014; Mazzoni et al., 2013; Thaler et al., 2002). In a subset of spinal commissural neurons, Lhx2 and Lhx9 act in parallel to promote midline crossing through upregulation of *Rig-1/Robo3* (Wilson et al., 2008). In *Drosophila* dorsally projecting motor neurons, Eve, Zfh1, and Grain act in parallel to promote the expression of *unc5*, *beat1a*, and *fas2*, although Eve also regulates additional targets important for axon guidance that are not shared by Zfh1 or Grain (Zarin et al., 2012, 2014).

Here we show that Isl and Hb9 act in parallel through at least two distinct effectors and propose that they regulate their targets by different mechanisms. Hb9 likely indirectly promotes *robo2* expression by repressing one or multiple intermediate targets because its conserved Engrailed homology repressor domain is required for its function in motor axon guidance and for *robo2* regulation (Santiago et al., 2014). In vertebrate motor neurons, Isl1 forms a complex with Lhx3 to directly activate several of its known targets (Cho et al., 2014; Lee et al., 2016; Thaler et al., 2002). A recent genome-wide DAM-ID analysis found that Isl binds to multiple regions within and near the *fra* locus in *Drosophila* embryos, suggesting that it may directly activate *fra* (Wolfram et al., 2014; Figure S1). Our finding that *lim3* is not required for *fra* expression in RP motor neurons, together with evidence that Isl can alter the electrical properties of muscle cells independently of Lim3, suggest that *Drosophila* Isl does not need to form a complex with Lim3 for all of its functions (Wolfram et al., 2014). Future research will be necessary to detect Isl binding events in embryonic motor neurons, although these experiments are challenging when binding occurs transiently or in a small number of cells (Agelopoulos et al., 2014). Interestingly, overexpression of Isl using *ap-Gal4* or *hb9-Gal4* induces *fra* only in certain subsets of these neurons, consistent with a model in which Isl binds to the *fra* locus in a cell-type-specific manner (Figure 2; data not shown). The generation of many large-scale datasets for transcription factor binding sites presents the field with the task of reconciling these data with clearly defined genetic relationships during specific biological processes (Lacin et al., 2014; Mazzoni et al., 2013; Wolfram et al., 2014). Our study and others have initiated this effort, but it will be important to investigate the functional significance of other putative transcription factor-effector relationships to achieve a better understanding of how transcriptional regulators control cell fate (Cho et al., 2014; Hattori et al., 2013; Lodato et al., 2014; Wolfram et al., 2012).

EXPERIMENTAL PROCEDURES

Genetics

All crosses were carried out at 25°C. Embryos were genotyped using balancer chromosomes carrying *lacZ* markers or by the presence of epitope-tagged transgenes. Transgenic *UAS-Isl5xMyc* flies were generated by BestGene using ΦC31-directed site-specific integration into landing sites at cytological position 86Fb. See Supplemental Experimental Procedures for a list of mutant alleles used in this study.

Immunofluorescence and Imaging

Dechorionated, formaldehyde-fixed, methanol-devittellinized embryos were fluorescently stained using standard methods (see Supplemental Experimental Procedures for a list of antibodies used). Embryos were mounted in 70% glycerol/PBS. Fluorescent mRNA in situ hybridization was performed as described previously with a digoxigenin-labeled probe (Santiago et al., 2014). The *fra* antisense probe was transcribed from linearized cDNA cloned into pBluescript. Fluorescence quantification was performed as described previously (Santiago et al., 2014). Images were acquired using a spinning disk confocal system (PerkinElmer) built on a Nikon Ti-U inverted microscope using a Nikon OFN25 60× objective with a Hamamatsu C10600-10B charge-coupled device (CCD) camera and Yokogawa CSU-10 scanner head with Volocity imaging software. Max projections were generated, cropped, and processed using ImageJ.

Single-Cell Labeling

Embryos containing *hsFLP*, *UAS-FRTstopFRT-mCD8-GFP*, and *lim3b-Gal4* transgenes were collected overnight at 25°C in standard cages. Embryos were heat-shocked at 37°C the next morning for 3–5 min (FLP.122) or 45–60 min (FLP.12). Embryos were fixed 9 hr after H.S. using standard procedures. See Supplemental Experimental Procedures for additional details on phenotypic quantification.

Statistics

For statistical analysis, comparisons were made between genotypes using Student's t test or Fisher's exact test, as appropriate. For multiple comparisons, a post hoc Bonferroni correction was applied. Outliers were not excluded from statistical analyses. Sample sizes are indicated in the figures or figure legends.

SUPPLEMENTAL INFORMATION

Supplemental Information includes Supplemental Experimental Procedures, four figures, and four movies and can be found with this article online at http://dx.doi.org/10.1016/j.celrep.2017.01.041.

AUTHOR CONTRIBUTIONS

Conception and Design, C.S. and G.J.B.; Investigation, Analysis, and Writing – Original Draft, C.S.; Writing – Review and Editing, C.S. and G.J.B.; Resources and Supervision, G.J.B.

ACKNOWLEDGMENTS

We thank members of the Bashaw lab for their comments during the development of this manuscript. We thank Richard Baines and Tony Southall for help with processing and visualizing the DAM-ID data presented in Figure S1. C.S. was supported by an NSF pre-doctoral training grant (DGE-0822). This work was supported by NIH Grants R01NS-046333 and R01NS-054739 (to G.J.B.).

Received: September 12, 2016
Revised: November 30, 2016
Accepted: January 18, 2017
Published: February 14, 2017

REFERENCES

Agelopoulos, M., McKay, D.J., and Mann, R.S. (2014). cgChIP: A cell type- and gene-specific method for chromatin analysis. In Hox Genes: Methods and Protocols, Y. Graba and R. Rezsohazy, eds. (Humana Press), pp. 291–306.

Allan, D.W., Park, D., St Pierre, S.E., Taghert, P.H., and Thor, S. (2005). Regulators acting in combinatorial codes also act independently in single differentiating neurons. Neuron *45*, 689–700.

Baek, M., and Mann, R.S. (2009). Lineage and birth date specify motor neuron targeting and dendritic architecture in adult Drosophila. J. Neurosci. *29*, 6904–6916.

Brankatschk, M., and Dickson, B.J. (2006). Netrins guide Drosophila commissural axons at short range. Nat. Neurosci. *9*, 188–194.

Brierley, D.J., Blanc, E., Reddy, O.V., Vijayraghavan, K., and Williams, D.W. (2009). Dendritic targeting in the leg neuropil of Drosophila: the role of midline signalling molecules in generating a myotopic map. PLoS Biol. *7*, e1000199.

Broadie, K.S., and Bate, M. (1993). Development of the embryonic neuromuscular synapse of Drosophila melanogaster. J. Neurosci. *13*, 144–166.

Broihier, H.T., and Skeath, J.B. (2002). Drosophila homeodomain protein dHb9 directs neuronal fate via crossrepressive and cell-nonautonomous mechanisms. Neuron *35*, 39–50.

Catela, C., Shin, M.M., and Dasen, J.S. (2015). Assembly and function of spinal circuits for motor control. Annu. Rev. Cell Dev. Biol. *31*, 669–698.

Certel, S.J., and Thor, S. (2004). Specification of Drosophila motoneuron identity by the combinatorial action of POU and LIM-HD factors. Development *131*, 5429–5439.

Cho, H.-H., Cargnin, F., Kim, Y., Lee, B., Kwon, R.-J., Nam, H., Shen, R., Barnes, A.P., Lee, J.W., Lee, S., and Lee, S.K. (2014). Isl1 directly controls a cholinergic neuronal identity in the developing forebrain and spinal cord by forming cell type-specific complexes. PLoS Genet. *10*, e1004280.

Corty, M.M., Matthews, B.J., and Grueber, W.B. (2009). Molecules and mechanisms of dendrite development in Drosophila. Development *136*, 1049–1061.

Couton, L., Mauss, A.S., Yunusov, T., Diegelmann, S., Evers, J.F., and Landgraf, M. (2015). Development of connectivity in a motoneuronal network in Drosophila larvae. Curr Biol. *25*, 568–576.

Eade, K.T., Fancher, H.A., Ridyard, M.S., and Allan, D.W. (2012). Developmental transcriptional networks are required to maintain neuronal subtype identity in the mature nervous system. PLoS Genet. *8*, e1002501.

Evans, T.A., Santiago, C., Arbeille, E., and Bashaw, G.J. (2015). Robo2 acts in trans to inhibit Slit-Robo1 repulsion in pre-crossing commissural axons. eLife *4*, e08407.

Flames, N., and Hobert, O. (2009). Gene regulatory logic of dopamine neuron differentiation. Nature *458*, 885–889.

Fujioka, M., Lear, B.C., Landgraf, M., Yusibova, G.L., Zhou, J., Riley, K.M., Patel, N.H., and Jaynes, J.B. (2003). Even-skipped, acting as a repressor, regulates axonal projections in Drosophila. Development *130*, 5385–5400.

Furrer, M.-P., Kim, S., Wolf, B., and Chiba, A. (2003). Robo and Frazzled/DCC mediate dendritic guidance at the CNS midline. Nat. Neurosci. *6*, 223–230.

Furrer, M.-P., Vasenkova, I., Kamiyama, D., Rosado, Y., and Chiba, A. (2007). Slit and Robo control the development of dendrites in Drosophila CNS. Development *134*, 3795–3804.

Hattori, Y., Usui, T., Satoh, D., Moriyama, S., Shimono, K., Itoh, T., Shirahige, K., and Uemura, T. (2013). Sensory-neuron subtype-specific transcriptional programs controlling dendrite morphogenesis: genome-wide analysis of Abrupt and Knot/Collier. Dev. Cell *27*, 530–544.

Hobert, O. (2015). Terminal Selectors of Neuronal Identity, First Edition (Elsevier Inc.).

Kania, A., and Jessell, T.M. (2003). Topographic motor projections in the limb imposed by LIM homeodomain protein regulation of ephrin-A:EphA interactions. Neuron *38*, 581–596.

Keleman, K., Rajagopalan, S., Cleppien, D., Teis, D., Paiha, K., Huber, L.A., Technau, G.M., and Dickson, B.J. (2002). Comm sorts robo to control axon guidance at the Drosophila midline. Cell *110*, 415–427.

Kim, S., and Chiba, A. (2004). Dendritic guidance. Trends Neurosci. *27*, 194–202.

Kolodziej, P.A., Timpe, L.C., Mitchell, K.J., Fried, S.R., Goodman, C.S., Jan, L.Y., and Jan, Y.N. (1996). frazzled encodes a Drosophila member of the DCC immunoglobulin subfamily and is required for CNS and motor axon guidance. Cell *87*, 197–204.

Komiyama, T., Johnson, W.A., Luo, L., and Jefferis, G.S. (2003). From lineage to wiring specificity. POU domain transcription factors control precise connections of Drosophila olfactory projection neurons. Cell *112*, 157–167.

Kratsios, P., Stolfi, A., Levine, M., and Hobert, O. (2011). Coordinated regulation of cholinergic motor neuron traits through a conserved terminal selector gene. Nat. Neurosci. *15*, 205–214.

Labrador, J.P., O'keefe, D., Yoshikawa, S., McKinnon, R.D., Thomas, J.B., and Bashaw, G.J. (2005). The homeobox transcription factor even-skipped regulates netrin-receptor expression to control dorsal motor-axon projections in Drosophila. Curr. Biol. *15*, 1413–1419.

Lacin, H., Rusch, J., Yeh, R.T., Fujioka, M., Wilson, B.A., Zhu, Y., Robie, A.A., Mistry, H., Wang, T., Jaynes, J.B., and Skeath, J.B. (2014). Genome-wide identification of Drosophila Hb9 targets reveals a pivotal role in directing the transcriptome within eight neuronal lineages, including activation of nitric oxide synthase and Fd59a/Fox-D. Dev. Biol. *388*, 117–133.

Landgraf, M., Bossing, T., Technau, G.M., and Bate, M. (1997). The origin, location, and projections of the embryonic abdominal motorneurons of Drosophila. J. Neurosci. *17*, 9642–9655.

Landgraf, M., Roy, S., Prokop, A., VijayRaghavan, K., and Bate, M. (1999). Even-skipped determines the dorsal growth of motor axons in Drosophila. Neuron *22*, 43–52.

Landgraf, M., Jeffrey, V., Fujioka, M., Jaynes, J.B., and Bate, M. (2003). Embryonic origins of a motor system: motor dendrites form a myotopic map in Drosophila. PLoS Biol. *1*, E41.

Lee, B., Lee, S., Agulnick, A.D., Lee, J.W., and Lee, S.K. (2016). Single-stranded DNA binding proteins are required for LIM-complexes to induce transcriptionally active chromatin and specify spinal neuronal identities. Development *143*, 1721–1731.

Lefebvre, J.L., Sanes, J.R., and Kay, J.N. (2015). Development of dendritic form and function. Annu. Rev. Cell Dev. Biol. *31*, 741–777.

Livet, J., Sigrist, M., Stroebel, S., De Paola, V., Price, S.R., Henderson, C.E., Jessell, T.M., and Arber, S. (2002). ETS gene Pea3 controls the central position and terminal arborization of specific motor neuron pools. Neuron *35*, 877–892.

Lodato, S., Molyneaux, B.J., Zuccaro, E., Goff, L.A., Chen, H.-H., Yuan, W., Meleski, A., Takahashi, E., Mahony, S., Rinn, J.L., et al. (2014). Gene co-regulation by Fezf2 selects neurotransmitter identity and connectivity of corticospinal neurons. Nat. Neurosci. *17*, 1046–1054.

Lundgren, S.E., Callahan, C.A., Thor, S., and Thomas, J.B. (1995). Control of neuronal pathway selection by the Drosophila LIM homeodomain gene apterous. Development *121*, 1769–1773.

Luria, V., Krawchuk, D., Jessell, T.M., Laufer, E., and Kania, A. (2008). Specification of motor axon trajectory by ephrin-B:EphB signaling: symmetrical control of axonal patterning in the developing limb. Neuron *60*, 1039–1053.

Mauss, A., Tripodi, M., Evers, J.F., and Landgraf, M. (2009). Midline signalling systems direct the formation of a neural map by dendritic targeting in the Drosophila motor system. PLoS Biol. *7*, e1000200.

Mazzoni, E.O., Mahony, S., Closser, M., Morrison, C.A., Nedelec, S., Williams, D.J., An, D., Gifford, D.K., and Wichterle, H. (2013). Synergistic binding of transcription factors to cell-specific enhancers programs motor neuron identity. Nat. Neurosci. *16*, 1219–1227.

Mitchell, K.J., Doyle, J.L., Serafini, T., Kennedy, T.E., Tessier-Lavigne, M., Goodman, C.S., and Dickson, B.J. (1996). Genetic analysis of Netrin genes in Drosophila: Netrins guide CNS commissural axons and peripheral motor axons. Neuron *17*, 203–215.

Neuhaus-Follini, A., and Bashaw, G.J. (2015). The Intracellular Domain of the Frazzled/DCC Receptor Is a Transcription Factor Required for Commissural Axon Guidance. Neuron *87*, 751–763.

O'Donnell, M.P., and Bashaw, G.J. (2013). Src inhibits midline axon crossing independent of Frazzled/Deleted in Colorectal Carcinoma (DCC) receptor tyrosine phosphorylation. J. Neurosci. *33*, 305–314.

O'Donnell, M., Chance, R.K., and Bashaw, G.J. (2009). Axon growth and guidance: receptor regulation and signal transduction. Annu. Rev. Neurosci. *32*, 383–412.

Odden, J.P., Holbrook, S., and Doe, C.Q. (2002). Drosophila HB9 is expressed in a subset of motoneurons and interneurons, where it regulates gene expression and axon pathfinding. J. Neurosci. *22*, 9143–9149.

Palmesino, E., Rousso, D.L., Kao, T.-J., Klar, A., Laufer, E., Uemura, O., Okamoto, H., Novitch, B.G., and Kania, A. (2010). Foxp1 and lhx1 coordinate motor neuron migration with axon trajectory choice by gating Reelin signalling. PLoS Biol. *8*, e1000446.

Santiago, C., and Bashaw, G.J. (2014). Transcription factors and effectors that regulate neuronal morphology. Development *141*, 4667–4680.

Santiago, C., Labrador, J.-P., and Bashaw, G.J. (2014). The homeodomain transcription factor Hb9 controls axon guidance in Drosophila through the regulation of Robo receptors. Cell Rep. *7*, 153–165.

Syed, D.S., Gowda, S.B.M., Reddy, O.V., Reichert, H., and VijayRaghavan, K. (2016). Glial and neuronal Semaphorin signaling instruct the development of a functional myotopic map for Drosophila walking. eLife *5*, e11572.

Thaler, J.P., Lee, S.-K., Jurata, L.W., Gill, G.N., and Pfaff, S.L. (2002). LIM factor Lhx3 contributes to the specification of motor neuron and interneuron identity through cell-type-specific protein-protein interactions. Cell *110*, 237–249.

Thor, S., and Thomas, J.B. (1997). The Drosophila islet gene governs axon pathfinding and neurotransmitter identity. Neuron *18*, 397–409.

Thor, S., Andersson, S.G.E., Tomlinson, A., and Thomas, J.B. (1999). A LIM-homeodomain combinatorial code for motor-neuron pathway selection. Nature *397*, 76–80.

Vrieseling, E., and Arber, S. (2006). Target-induced transcriptional control of dendritic patterning and connectivity in motor neurons by the ETS gene Pea3. Cell *127*, 1439–1452.

Wilson, S.I., Shafer, B., Lee, K.J., and Dodd, J. (2008). A molecular program for contralateral trajectory: Rig-1 control by LIM homeodomain transcription factors. Neuron *59*, 413–424.

Wolfram, V., Southall, T.D., Brand, A.H., and Baines, R.A. (2012). The LIM-homeodomain protein islet dictates motor neuron electrical properties by regulating K(+) channel expression. Neuron *75*, 663–674.

Wolfram, V., Southall, T.D., Günay, C., Prinz, A.A., Brand, A.H., and Baines, R.A. (2014). The transcription factors islet and Lim3 combinatorially regulate ion channel gene expression. J. Neurosci. *34*, 2538–2543.

Zarin, A.A., Daly, A.C., Hülsmeier, J., Asadzadeh, J., and Labrador, J.-P. (2012). A GATA/homeodomain transcriptional code regulates axon guidance through the Unc-5 receptor. Development *139*, 1798–1805.

Zarin, A.A., Asadzadeh, J., Hokamp, K., McCartney, D., Yang, L., Bashaw, G.J., and Labrador, J.-P. (2014). A transcription factor network coordinates attraction, repulsion, and adhesion combinatorially to control motor axon pathway selection. Neuron *81*, 1297–1311.